ACS APPLIED MATERIALS & INTERFACES

Research Article

www.acsami.org

Perfluorinated Polymer Electrolytes Hybridized with In situ Grown Titania Quasi-Networks

Yatin Patil,[†] Satheesh Sambandam,[‡] Vijay Ramani,*[,‡] and Kenneth Mauritz[†]

[†]School of Polymers and High Performance Materials, University of Southern Mississippi, 118 College Drive, Box # 10076, Hattiesburg, Mississippi 39406, United States (USA) E-mail: kenneth.mauritz@usm.edu

[‡]Department of Chemical and Biological Engineering, Illinois Institute of Technology, 10 W 33rd Street; 127 PH, Chicago, Illinois 60616, United States

Supporting Information

ABSTRACT: Perfluorinated Nafion membranes, neutralized to various extents, were hybridized with titania quasi-networks that were grown in situ via catalyzed sol–gel reactions of an titanium isopropoxide precursor. The formation of Ti–O–Ti groups within the ionomer was verified by FTIR-ATR spectroscopy. EDAX studies confirmed that the extent of propagation of titania quasi-networks into the bulk of the ionomer film increased with ionomer neutralization. Compared to the unmodified control membrane, the hybrid membranes exhibited superior dimensional stability, modulus, stress, and strain at break and gas barrier properties. All hybrid membranes exhibited superior resistance to degradation when subjected to an accelerated stress test in an operating fuel cell environment, as a resultant of the better dimensional stability and gas barrier properties induced through addition of the inorganic titania phase.

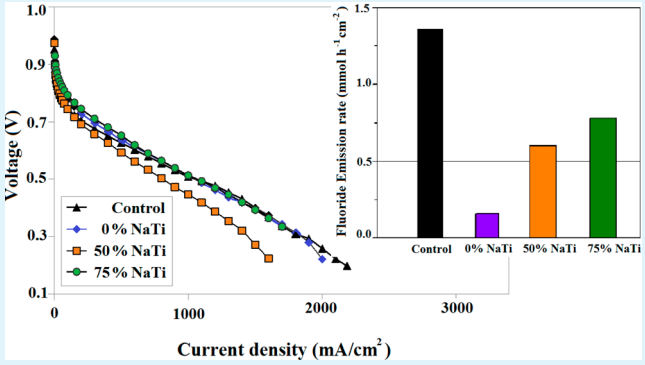

KEYWORDS: *perfluorinated ionomers, titania quasi-networks, polymer electrolyte fuel cells, in situ sol–gel*

1. INTRODUCTION

The nanophase-separated morphology of Nafion membranes – comprising hydrophilic clusters within a hydrophobic matrix – has been exploited as a morphological template for in situ growth of inorganic quasi-networks via sol–gel reactions of alkoxide monomers such as tetraethoxysilane [TEOS = $Si(OC_2H_5)_4$], diethoxydimethylsilane [DEDMS = $(CH_3)_2Si(OC_2H_5)_2$] and TEOS-DEDMS mixtures to create Nafion/SiO_2, Nafion/dimethylsiloxane and Nafion/[organically modified silicate] hybrid materials.[1] Nafion is a perfluorosulfonate ionomer whose general morphology consists of 3–5 nm sized clusters of —SO_3H ended perfluoroalkylether side chains that are dispersed throughout a semicrystalline tetrafluoroethylene matrix. For an alcohol-swollen Nafion membrane, hydrolyzed silicon alkoxide monomers migrate to the clusters, which serve as nanoreactors within which sol–gel reactions occur, catalyzed by fixed SO_3H groups tethered to the polymer side-chain. Small-angle X-ray scattering studies of these hybrid membranes have established that the original morphology of unfilled Nafion was unchanged after sol–gel modification, confirming that the Nafion acts as an interactive template that directs the morphological disposition of the inorganic phase.[2] Mechanical tensile studies showed classical percolation behavior of the silicon oxide phase when proceeding from low to high filler levels, which was characterized by a ductile-to-brittle transformation.[3] The ability to insert such inorganic quasi-networks into a perfluorinated ionomer offers a simple way to enhance the mechanical and barrier properties of these materials, which have widespread applications as polymer electrolyte membranes (PEMs) used in polymer electrolyte fuel cells (PEFCs) and electrolyzers.

PEFCs have been extensively researched as a chemical-to-electrical energy conversion device for a variety of applications, ranging from automotive engines to portable power. PEFCs incorporate a thin catalyst coated PEM, typically a perfluorinated material such as Nafion, that conducts protons, prevents reactant gas (H_2, O_2/air) crossover, withstands mechanical degradation due to stresses generated during fuel cell operation, and withstands chemical (oxidative) degradation induced by free radical reactive oxygen species that are generated during fuel cell operation, usually via a peroxide intermediate.[4−8] Nafion remains the benchmark PEM in fuel cell research and its structure and properties have been exhaustively reviewed by Mauritz and Moore.[9] Although Nafion possesses excellent properties, its high cost and relatively poor durability remain significant barriers for their use in PEFCs. The critical factors limiting the durability/lifetime of a Nafion in a fuel cell are crack and pinhole formation and concomitant oxidative

Received: August 25, 2012
Accepted: December 4, 2012
Published: December 4, 2012

 © 2012 American Chemical Society

degradation, which are attributed to the combined action of physical (mechanical) and chemical degradation.[10,11]

Physical degradation of Nafion membranes can be largely attributed to the poor dimensional stability of the membrane. The dimensional change due to an increase in relative humidity (synonymous with extent of PEM hydration) from 0 to 100% at fuel cell operating temperatures can be as high as 15−20%.[12] Different degrees of PEM hydration are encountered during fuel cell operation as a consequence of relative humidity and temperature variations that arise during transients (start−stop) and changes in current density.[13] Water activity gradients across the mechanically constrained membrane electrode assemblies (MEAs) can cause differential swelling, which generates internal stresses that contribute to membrane failure. Poor dimensional stability weakens the membrane and accelerates the rate of fuel and oxidant crossover across the membrane due to the formation of pinholes or cracks. Fuel/oxidant crossover across the PEM results in a much increased rate of hydrogen peroxide formation, and consequently a much greater concentration of oxidative-degradation-inducing free radical ROS such as hydroxyl and hydroperoxyl radicals.[14] Various studies support the contention that the crossover of hydrogen and oxygen toward opposite electrodes is responsible for generating the ROS contributing to membrane oxidative degradation.[15−18]

Physical and chemical degradation in a Nafion membrane during fuel cell operation are synergistic processes. The root causes for said degradation are the poor dimensional stability of the membrane and its poor gas barrier properties, especially at the hydrated interconnected ionic clusters, which provide paths of least resistance to gas diffusion.[19] When hydrated, the membrane structure expands, creating multiple pathways for fuel and oxidant diffusion toward the opposite electrodes.[20] The water-swollen (hydrated) regions of low mechanical modulus, located adjacent to drier, hydrophobic regions of higher modulus are postulated to be the loci of membrane failure, owing to differential swelling stresses that arise at the interface. During fuel cell operation, these regions continuously weaken because of reduced ductility and reduced molecular weight arising from chemical attack by free radicals, resulting in larger defect features.[21] The increase in defect size further exacerbates the situation by allowing for more rapid gas crossover and more rapid generation of oxidative-degradation-inducing ROS. The process is therefore autocatalytic in nature, with a certain induction time. The situation is analogous to environmental stress cracking, wherein the reactive environment in this case contains hydroxyl radicals, and the constrained membrane experiences stresses due to changes in temperature and relative humidity. This degradation process will continue until most of the weak regions eventually form pinholes, resulting in catastrophic failure. By reducing gas crossover, and by increasing the mechanical properties at the interface between the hydrophobic and hydrophilic domains, the rate of both physical and chemical degradation process can be significantly lowered.

Inserting nanoscopic particles that obstruct the gas diffusion pathways can reduce gas crossover through the ionomer membrane. Furthermore, particles that are slightly interconnected through metal (in this case, titanium) oxide bonds form a load-bearing network that simultaneously enhances mechanical properties. Our previous work involving in situ generation of stable titania quasi-networks in Nafion membranes yielded membranes demonstrating improved dimensional stability and enhanced mechanical and gas barrier properties that significantly retarded their physical and chemical degradation.[22] Fuel cell performance, after subjecting these hybrid membranes to accelerated degradation tests, was unchanged, whereas that of an unmodified Nafion membrane deteriorated severely.

Although this inorganic sol−gel modification retarded membrane degradation, it resulted in reduced fuel cell performance due to decrease in proton conductivity. It was envisioned that the excluded volume posed by the inorganic oxide quasi-networks in the polar clusters decreased membrane water uptake, restricted polymer chain mobility and increased tortuosity for proton migration. Another issue that was encountered was that the growth of the inorganic phase was quite pronounced close to the membrane surface, but less so in the bulk of the membrane. This nonhomogeneity was attributed to the rapid formation of the inorganic phase at the surface of the membrane, catalyzed by the sulfonic acid groups at the surface. This surface/subsurface layer precluded further diffusion of precursor into the bulk of the film, resulting in a gradient in the distribution of the inorganic phase.

This study reports the effect of partial neutralization of sulfonic acid groups in the Nafion membrane on the structure and properties of the resultant hybrid membranes containing *in situ* grown titania quasi-networks. It is postulated that the neutralization process will retard the rate of formation of the surface layer, permitting a more uniform distribution of the inorganic phase within the ionomer bulk. Note that in this discussion, the term 'quasi-network' refers to condensed titanium oxide hyperbranched structures of limited sizes as opposed to macroscopic percolated networks. These structures may be interknitted to a limited degree by Ti−O−Ti links. Although the word "titania" usually refers to a pure macroscopic material having chemical composition TiO_2, here it refers to the incompletely condensed quasi-networks dispersed throughout the ionomer matrix.

2. RESULTS AND DISCUSSION

2.1. Inorganic Weight Uptake and Hybrid Membrane Characterization. The difference between the dried weight of the membrane after nitric acid cleaning and the weight after sol−gel treatment followed by acid−water cleaning was considered as the titania uptake. The control sample lost 1.2% of its initial weight, due to low molecular weight polymer fragments being leached out into the alcohol solution during membrane swelling. The titania weight uptakes for 0%NaTi, 50%NaTi, and 75%NaTi membranes were 12.1, 13.4, and 12.4%, respectively, which allowed for good comparison of results. The fixed sulfonic acid groups catalyzed the sol−gel reaction of $Ti(iOPr)_4$ within the ionic clusters. The titania uptake did not decrease with increasing acid neutralization despite the lack of acid catalytic sites. This was attributed to the presence of water, which hydrolyzed $Ti(iOPr)_4$ to $Ti(OH)_4$. The hydrolysis was followed by Ti−O−Ti bond formation by condensation reactions that facilitated particle/network growth. Although anhydrous methanol was used as the reaction media, neutralization of sulfonic acid generated equivalent moles of water that promoted the sol−gel reactions. Thus, the 0% NaTi membrane had high acid content but low water content, whereas at the other extreme the 75% NaTi membrane had low acid content but high water content. The effective equivalent weights of Nafion, and 0%NaTi, 50% NaTi, and 75% NaTi membranes were measured to be 1107, 1122, 1063, and 1074 g/mol, respectively. This indicated that the incorporated sol−gel-derived titania quasi-networks did not diminish the effective

dx.doi.org/10.1021/am3017834 | ACS Appl. Mater. Interfaces 2013, 5, 42−48

concentration of ion exchange sites. Additional information presented under electronic Supporting Information: (a) a discussion of the characterization of the hybrid membranes by FTIR-ATR spectroscopy (Figure S1 and accompanying discussion); (b) a discussion of the distribution of the inorganic phase within the ionomer, as measured by EDAX (Figure S2 and accompanying discussion); **c)** Water uptake of the hybrid membranes (Figure S3 and accompanying discussion)

2.2. Mechanical Properties of Hybrid Membranes. Mechanical tensile stress vs strain curves for the control sample and the titania-modified hybrid membranes at 80 °C, measured using a dynamic mechanical analyzer without humidity control, are displayed in Figure 1. These membranes all had very low

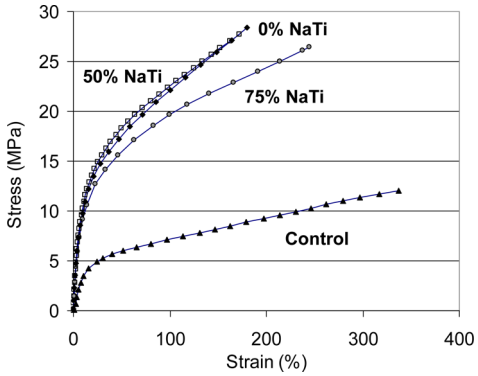

Figure 1. Mechanical tensile stress–strain curves for the unfilled Nafion control, 0% NaTi, 50% NaTi, and 75% NaTi Nafion/titania membranes at 80 °C.

water content during the measurement, as there was no provision for humidification in the chamber. The curves for all the three hybrid membranes were considerably elevated above that of the unfilled Nafion control membrane at all strains. This unequivocally confirmed that the incorporation of titania quasi-networks improved the mechanical properties of Nafion. The average tensile properties of three runs for each membrane are listed in Table 1. The standard error was on the order of 10%

Table 1. Mechanical Tensile Properties of an Unfilled Nafion Control and 0% NaTi, 50% NaTi, and 75% NaTi Nafion/Titania Membranes at 80 °C[a]

	control	0% NaTi	50% NaTi	75% NaTi
modulus (MPa)	60.4	191.2	192.9	165.1
stress at break (MPa)	11.6	28.9	26.3	25.6
strain at break (mm/mm)	315.7	220.5	162.4	245.7

[a]Average values are shown, with a standard error of 10%.

for these measurements. The hybrid membranes exhibited much higher modulus (2.5–3 fold higher) and stress-at-break (2–2.5 times higher) than the control sample, indicating superior mechanical properties. The strain-at-break was lower for the hybrid membranes when compared to the control sample. The strain-at-break reflects degree of brittleness and the lower value for the hybrid membranes was attributed to both short-range perfluoro-organic/inorganic filler interactions and to the degree of interconnectivity of the titania quasi-networks. The strain-at-break was greatest for the control sample because there were no polymer–particle interactions or titania structures interknitted by Ti–O–Ti bonds; rather, deformation at high strain occurred only by slippage of polymer chains through their entanglements and perhaps by disruption of small regions of limited crystallinity.

The rate at which TiOH + TiOH → Ti–O–Ti + H_2O condensation reactions proceeded relative to the diffusion speed of titanium isopropoxide: 2,4-pentanedione complexes governed the distribution of the inorganic phase in the membrane (see also Figure S2 in the Supporting Information). In the non-neutralized 0% NaTi membrane, the rate of condensation was higher than that of precursor diffusion into the bulk, resulting in better load bearing networks at the surface. Sulfonic acid group neutralization, the degree of which decreased from the surface inward, permitted the precursor complex to diffuse deeper into the membrane prior to condensation resulting in a less interconnected, but more uniformly distributed network, as reflected by the trends seen in modulus and strain-at-break for the hybrid membranes (Table 1).

Figure 2 shows the stress–strain curves for the Nafion control and the Nafion/titania hybrid membranes at the normal

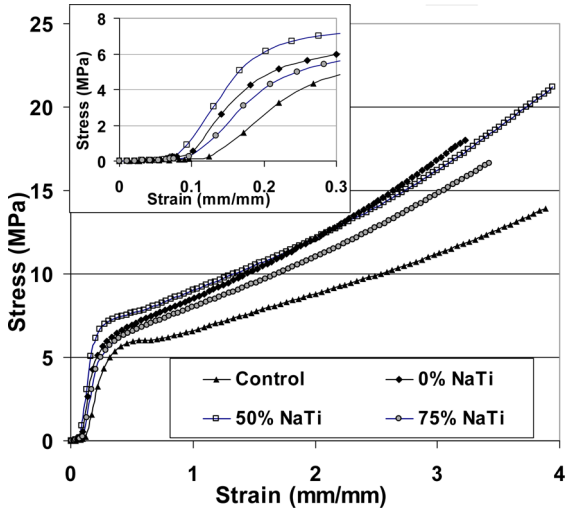

Figure 2. Mechanical tensile stress–strain curves for an unfilled Nafion control and 0% NaTi, 50% NaTi, and 75% NaTi Nafion/titania membranes at 80 °C and 100% RH. The inset is a magnification of the initial strain region.

fuel cell operating temperature of 80 °C. The samples were first conditioned for 2h at 80 °C and 100% RH in a custom designed environmental chamber. Following this, the membranes were stretched at 5 mm/min to their strains-at-break, generating the curves in Figure 2. The initial horizontal strain displacement that took place with no counteractive stress was due to sample expansion on swelling during conditioning. The load cell did not register force until the sample reached its taut length and the displacement until this point provided a measure of sample dimensional change. The inset in Figure 2 shows a magnified view of the initial strain region up to the sample displacement at which the stress began to rise. On the basis of this data, it was deduced that the hybrid membranes exhibited diminished swelling due to the reinforcement provided by the inorganic phase. Thus, the introduction of inorganic quasi-networks improved dimensional stability, a positive attribute for fuel cell membranes. The bar graph in Figure 3 summarizes the average mechanical tensile properties of three runs for control and the hybrid membranes derived from the stress–strain data in Figure 2. The hybrid membranes all exhibited a modest

dx.doi.org/10.1021/am3017834 | ACS Appl. Mater. Interfaces 2013, 5, 42–48

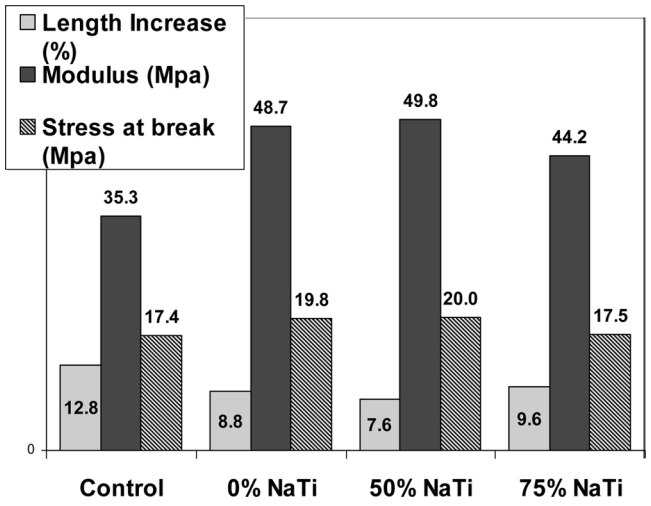

Figure 3. Mechanical tensile properties of an unfilled Nafion control and 0% NaTi, 50% NaTi, and 75% NaTi Nafion/titania membranes at 80 °C, and 100% RH. Average values are plotted, with a standard error of 10%.

increase in modulus over the control. The value of modulus was significantly lower than that measured under dry conditions. This was attributed to the fact that the absorbed water acted as a plasticizer that was mainly effective in the polar regions. Thus, the titania reinforcement was most beneficial in improving the dimensional stability of the hybrid membranes at elevated temperature and humidity, as manifested by the reduced dimensional change on humidification. The extent of enhancement of dimensional stability was governed by the extent of particle interconnectivity for a similar titania uptake.

Figure 4 shows contractile stresses developed in clamped samples at 80 °C for the control and hybrid membranes that

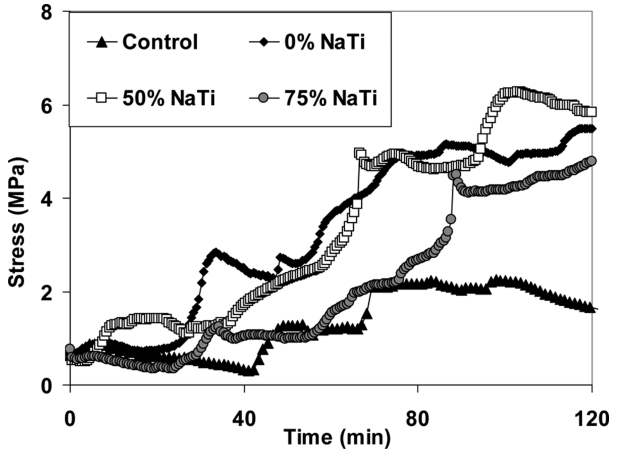

Figure 4. Contractile stress vs time response to RH drop from 100 to 0% at 80 °C for the control and 0% NaTi, 50% NaTi, and 75% NaTi Nafion/titania membranes that were clamped at constant length.

were subjected to a drop in humidity from 100% to 0% RH. All membranes eventually yielded, presumably by chain slippage under stress, and additionally in the case of the filled membranes, by rupture of the polymer–particle interactions. The unfilled Nafion control yielded at a stress of 2.2 MPa while the hybrid membranes offered better resistance to deformation with higher stresses at yield. The improved resistance was attributed to strong particle–polymer interactions and the disproportionate enhancement in modulus in the hybrid membranes as the films dried. It was observed that the samples, including the control, underwent a series of stress rises and declines superimposed on the overall trends. It is believed that this series of peaks arise because of a sequence of noncatastrophic crazes spanned by fibrils that prevent further damage growth in the region. This phenomenon has been observed in earlier studies[22] and verified by examining post-test SEM micrographs of the damage zones.

2.3. Chemical Degradation–Fluoride Emission Rate (FER). Figure 5 shows the combined FER generated at the

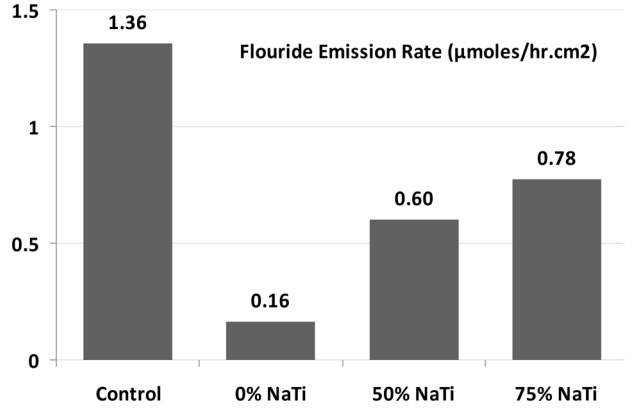

Figure 5. Fluoride emission rates for the unfilled Nafion control and the 0% NaTi, 50% NaTi, and 75% NaTi Nafion/titania membranes after the OCV test. Average values are plotted, with a standard error of 10%.

anode and cathode from MEAs prepared with the control and the three hybrid membranes. The FER data was collected after 24h of accelerated OCV testing. The control exhibited the highest FER, indicating highest extent of oxidative degradation due to poor gas barrier properties. The 0% NaTi membrane showed the lowest FER among the three hybrid membranes, in agreement with the voltage decay results of the OCV test (see Figure S5 in the Supporting Information). It is postulated that the better interconnectivity of titania particles for this hybrid minimized the gas crossover rate, which in turn retarded the rate of ROS formation, thereby lowering membrane chemical degradation through •OH radical attack.

Linear sweep voltammetry was performed to measure the hydrogen crossover current (flux) through the membrane (see Figure 6). The measured crossover current was 1 mA/cm^2 for the unfilled Nafion control and decreased to 0.71–0.75 mA/cm^2 for the 0% NaTi and 50% NaTi Nafion/titania membranes; 75%NaTi composite membrane had a crossover current of 0.85 mA/cm^2. The crossover currents were lower for the MEAs that exhibited lower FER, confirming that the macroscopic membrane degradation rate (FER) was related to gas crossover/permeability. Lower gas permeability resulted in less hydrogen peroxide formation and consequently in lower macroscopic degradation rates.

Another factor that accounts for the reduction in the macroscopic rate of membrane degradation is the ability of titania to serve as a hydrogen peroxide decomposition catalyst.[23] This ability of titania will lower hydrogen peroxide concentration locally within the membrane, resulting in a lower concentration of free radicals and hence lower FER. Compounds that can act as a hydrogen peroxide decomposition

dx.doi.org/10.1021/am3017834 | ACS Appl. Mater. Interfaces 2013, 5, 42–48

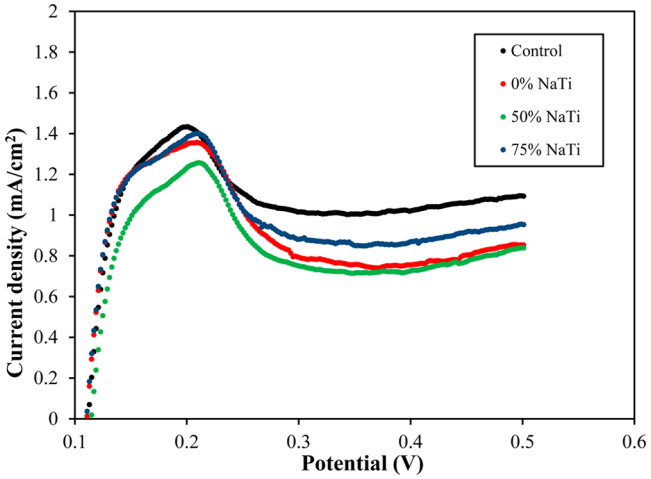

Figure 6. Linear sweep voltammetry for the unfilled Nafion control and the 0% NaTi, 50% NaTi, and 75% NaTi Nafion/titania membranes after the OCV test.

catalyst have been shown to decrease FER in fuel cells by 2−3 orders of magnitude.[5−8,23]

2.4. Fuel Cell Performance. Fuel cell performance curves, obtained before the accelerated OCV test, for MEAs prepared using the control and the three hybrid membranes are shown in Figure 7. Under similar catalyst loading, processing, and

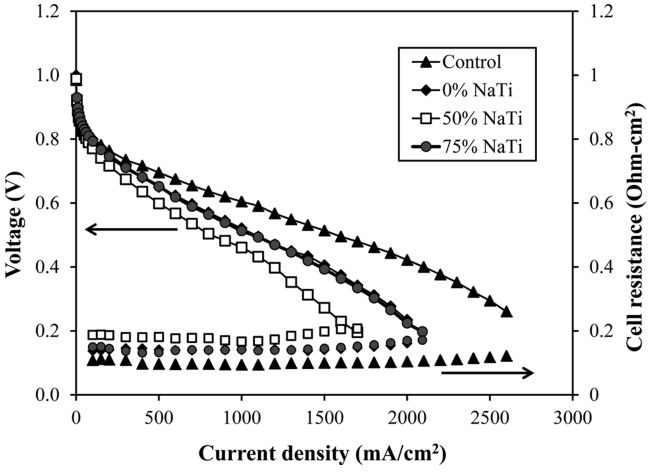

Figure 7. Polarization curves for control, 0% NaTi, 50% NaTi, and 75% NaTi Nafion/titania membranes before the OCV test at 80 °C and 75% RH.

operation conditions, the MEA performance depends on water uptake, proton conductivity and fuel crossover. High water uptake and high proton conductivity will improve fuel cell performance while high fuel crossover decreases performance and durability. The cell resistance in the operating fuel cells was between 0.1 and 0.2 ohm cm^2. The trends observed were the same that were observed for the conductivity of the composite membranes (ascertained via ex situ measurements). Nafion112 (control) had the lowest cell resistance of about 0.1 ohm cm^2), and 50% NaTi the highest cell resistance of almost 0.2 ohm cm^2 (see Figures 7 and 8).

The initial performance of unmodified Nafion was higher than that of all the three hybrid membranes. This was consistent with expectation, considering the higher water uptake and proton conductivity of the former (see Figure 9

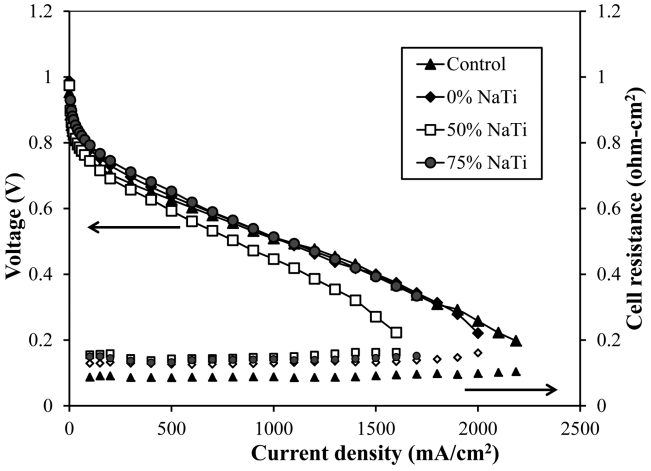

Figure 8. Polarization curves for an unfilled Nafion control and 0% NaTi, 50% NaTi, and 75% NaTi Nafion/titania membranes after the OCV test at 80 °C and 75% RH.

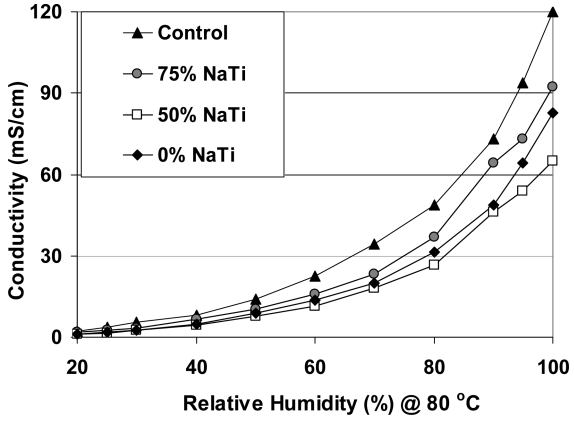

Figure 9. Conductivity vs RH for the unfilled Nafion control and the 0% NaTi, 50% NaTi, and 75% NaTi Nafion/titania membranes at 80 °C. Average values are plotted, with a standard error of 5%.

and Figure S4, Supporting Information) and the fact that degradation had not proceeded to a detrimental degree during the initial test (the degradation process has a significant induction time). Fuel cell performance curves that were acquired after the accelerated OCV test for the control and the three hybrid membranes are shown in Figure 8. The performances of the control and the 0% NaTi and 75% NaTi membranes were comparable at high current densities. However, at low current densities, the control Nafion membrane performed poorer than the two hybrid membranes. The inferior performance at low current densities for the control sample after the OCV test was attributed to the increased fuel crossover arising from increased defect formation in the absence of the reinforcing inorganic phase. The improved mechanical and barrier properties of the hybrid membranes enabled them to better withstand the harsh accelerated degradation test as well as the changes in relative humidity encountered between the initial and final performance tests. The 50% NaTi membrane performance was lower than the other hybrid variants because of its correspondingly lower water uptake and proton conductivity (this sample had the highest inorganic phase loading). Figures S6−S9 presented under electronic Supporting Information show the comparative fuel cell performance curves for the 0% NaTi, 50% NaTi, 75%

dx.doi.org/10.1021/am3017834 | ACS Appl. Mater. Interfaces 2013, 5, 42−48

NaTi and the control membrane before and after the accelerated OCV test. The hybrid membranes all exhibit similar performance before and after the accelerated test owing to superior resistance to mechanical and chemical degradation. On the other hand, the control sample showed extensive degradation in performance. This was consistent with prior results.[24]

The proton conductivity for the control and the three hybrid membranes at 80 °C are plotted against RH in Figure 9. The conductivity of the control was higher than that of all three hybrid membranes over the entire RH range. Recall that although incorporation of titania particles did not diminish equivalent weight, it did lower hydration capacity and swelling. Also, the dispersed titania particles increased the tortuosity of the proton migration pathways. All of these factors account for the reduced conductivity of the hybrid membranes seen in Figure 8. Among the three hybrids, conductivity was lowest for 50% NaTi and highest for 75% NaTi, which was in accordance with the comparative water uptakes.

3. CONCLUSIONS

Titania quasi-networks were incorporated into perfluorinated ionomer (Nafion) membranes via in situ catalyzed sol−gel reactions using titanium isopropoxide as a precursor. FTIR-ATR spectroscopy verified successful Ti−O−Ti bond formation. EDAX studies showed that the partial neutralization of sulfonic acid groups influenced the distribution of the titania networks in the thickness dimension. In a non-neutralized Nafion membrane, the titania structures formed initially in the near-surface regions, which then restricted diffusion of the precursor monomers toward the interior. This resulted in a U-shaped composition profile across the membrane thickness. In a partially neutralized membrane, the precursor monomer reached the interior and polymerized to a greater degree within the interior, resulting in a more uniform distribution.

The titania uptake for membranes with different degrees of neutralization and without neutralization were similar (at about 12 wt %). The mechanical properties of the hybrid membranes were much superior to that of the control when dry (2−3 fold enhancement). The variation in mechanical properties between the different hybrids suggested a modest influence of titania network interconnectivity on properties. The values of stress and strain at break were taken to be signatures of extent of particle interconnection. By this measure, interparticle connectivity in non-neutralized Nafion was highest while that in the partially neutralized membrane with highest amount of neutralization was lowest. Higher particle interconnectivity resulted in improved mechanical and gas barrier properties and better dimensional stability against humidity change. The titania networks, knitted together by Ti−O−Ti linkages, reinforced the membrane so as to better distribute stress and prevent or lower swelling. This significantly enhanced the dimensional stability (resistance to swelling) in hybrid membranes. However, the reduced water uptake also lowered membrane proton conductivity. This conclusion was supported by the fact that the hybrid membrane with lowest particle interconnectivity (75% NaTi) showed the highest water uptake and highest proton conductivity.

The initial fuel cell performances of all the three hybrid membranes were lower than that of the control because of lower water uptake and lower proton conductivity. However, the hybrid membranes exhibited superior durability as evidenced by their response to an accelerated stress test (OCV hold) and the humidity cycling encountered pre and post the OCV test. The poor dimensional stability of the control sample was attributed to excessive differential swelling stresses arising at the interface between the hydrophilic and hydrophobic phases during humidity and temperature cycling. The incorporation of well-dispersed inorganic networks mitigated the impact of these differential stresses and additionally decreased fuel crossover by increasing tortuosity. Thus, a simple sol−gel modification allowed significant durability enhancement in Nafion membranes by retarding both physical and chemical degradation.

4. EXPERIMENTAL SECTION

Membrane Cleaning and Hybrid Membrane Preparation. Nafion 112 membranes were cleaned by boiling in 8 M nitric acid for 2h followed by boiling in deionized water twice for 2h to leach out residuals. The membranes, after drying at 80 °C under vacuum for 24 h, were weighed to measure initial weight. Membranes were introduced in a flat bottom reaction chamber containing anhydrous methanol and were partially neutralized by adding a known amount of 0.05 N methanolic sodium hydroxide solution. The amount of sodium hydroxide required to achieve 50% and 75% acid neutralization was calculated assuming 1100 g/mol Nafion equivalent weight. Membranes, after swelling, were laid flat in the reaction chamber without any wrinkles or overlap. Titanium iso-propoxide $Ti(iPr)_4$ was used as the sol−gel precursor monomer and 2, 4-pentanedione was added as a complexing agent to reduce the otherwise rapid sol−gel reaction rate. A ratio of 1.5:1 for 2, 4-pentanedione: $Ti(iPr)_4$ was maintained. The mole fraction of $Ti(iPr)_4$ in the reaction mixture was 0.01. The membranes, after swelling for 24 h, were temporarily removed for ∼30 s, during which time 2, 4-pentanedione and the sol−gel precursor monomer were added and stirred to form a homogeneous reaction solution. Then, the membranes were reimmersed for 15 min and, after removal from the reaction mixture, washed quickly in methanol, and dried at 100 °C for 16h to promote condensation. After drying, the membranes were refluxed in 8 M HNO_3 for 2h followed by refluxing in deionized water twice for 1h each time to remove unreacted residuals. The membranes were then dried at 100 °C under vacuum for 24h. To study the influence of acid neutralization, a simultaneous sol−gel experiment was performed without any addition of sodium hydroxide (i.e., without neutralization). A control Nafion sample was subjected to similar processing conditions. Nafion membranes subjected to sol−gel modification without any neutralization is referred as 0%NaTi and those subjected to 50% and 75% neutralization are referred as 50%NaTi and 75%NaTi, respectively.

Mechanical Properties. The mechanical properties of membranes were studied using a TA Q800 dynamic mechanical analyzer without humidity control. The tensile properties of titania-modified and unmodified membranes at 80 °C and 100% RH were tested using an MTS Alliance RT/10 tensile setup equipped with a custom designed environmental chamber. The same equipment and test setup was used to study the build-up of contractile stresses developed in constrained membranes. To study the contractile stress build-up, samples were clamped in the tensile setup, were conditioned for 2h with an 80 °C, 100% RH nitrogen stream supplied at the rate of 0.3 L/min. After this conditioning, to hold the membrane at its extended swollen length due to water uptake, the crosshead position was slowly adjusted until the load cell detected a small tension of 0.1N. The crosshead position was then locked and the 100% RH stream was switched, at 0.3 L/min, to 0% RH nitrogen at 80 °C. The dry stream caused the membrane to dehydrate and the membrane attempted to contract to its original length. Because the sample was clamped at the swollen length, it exerted a contractile stress that was monitored vs time.

Membrane Electrode Assembly (MEA) Preparation. MEAs were prepared using 40% Pt/C (Alfa Aesar) as catalyst for both anode and cathode layers. Catalyst ink was prepared by mixing 0.2 g of catalyst, 1.7 g of 5% Nafion dispersion, and 7 mL of methanol. MEAs were prepared by spraying successive layers of catalyst ink directly

dx.doi.org/10.1021/am3017834 | ACS Appl. Mater. Interfaces 2013, 5, 42−48

onto either side of the membrane. An IR lamp was used to dry the MEA prior to the application of each layer. A PTFE mask was employed to maintain the MEA active area of 5 cm^2. After spraying of catalyst layers, the MEA was hot-pressed under 10 atm at 120 °C. The platinum loading at the anode was 0.2 mg cm^{-2} and that at the cathode was 0.4 $mg.cm^{-2}$. The MEAs were assembled in a 5 cm^2 fuel cell hardware containing serpentine flow fields (Fuel Cell Technologies Inc.). Two 375 μm thick gas diffusion layers (Sigracet 10BB) were used during assembly. The assembly was sealed using two 250 μm thick PTFE gaskets. All MEAs were tested on a Scribner Associates (Model 850C) fuel cell test station.

Fuel Cell Performance and Durability Experiments. Linear sweep voltammetry (LSV) was performed to investigate hydrogen crossover and electronic shorting in the MEA. Hydrogen and nitrogen at 80 °C, 75% RH, were passed through the anode and cathode side at flow rates of 200 mL/min. The working electrode (cathode) was swept from 0.05 to 0.8 V (vs SHE) at 4 mV s^{-1} and the current due to oxidation of crossover hydrogen was recorded.

Polarization curves were obtained at 80 °C and 75% inlet RH. Air as well as oxygen was used as oxidant (200 mL/min) and pure hydrogen was used as fuel (200 mL/min). The current was scanned from 0 A to the time when the cell voltage dropped below 0.2 V to obtain a sufficient number of points in the low and high current regime.

The MEAs were then subjected to an accelerated stress test. Each MEA was held under open circuit voltage (OCV) conditions at 100 °C and 25% RH. Oxygen was used as the oxidant (100 mL/min) and hydrogen was used as the fuel (100 mL/min). The test was run for 24 h for each MEA and the anode and cathode condensates were independently collected in cold traps. Fluoride ion concentrations in the condensate water were measured using a fluoride ion selective electrode (Denver Instruments) ,which was calibrated before each measurement. Following this accelerated test, the fuel cell performance and hydrogen crossover were determined.

■ ASSOCIATED CONTENT

Ⓢ Supporting Information

FTIR, EDAX, water uptake, proton conductvity, and additional experimental details. This material is available free of charge via the Internet at http://pubs.acs.org.

■ AUTHOR INFORMATION

Corresponding Author

*E-mail: ramani@iit.edu.

Notes

The authors declare no competing financial interest.

■ ACKNOWLEDGMENTS

The authors thank the United States Department of Energy, Office of Energy Efficiency and Renewable Energy (DE-FG36-08GO88106) for their support of this work. The authors thank the E.I. DuPont Co. for the Nafion samples. V.R. acknowledges support from the National Science Foundation (Grant # 0847030).

■ REFERENCES

(1) Mauritz, K. A.; Hassan, M. K. *Polym. Rev.* **2007**, *47*, 1−43.
(2) Deng, Q.; Cable, K. M.; Moore, R. B.; Mauritz, K. A. *J. Polym. Sci., Part B: Polym. Phys.* **1996**, *34* (11), 1917−1923.
(3) Young, S. K.; Mauritz, K. A. *J. Polym. Sci., Part B: Polym. Phys.* **2002**, *40* (19), 2237−2247.
(4) Trogadas, P.; Parrondo, J.; Ramani, V. *Electrochem. Solid-State Lett.* **2008**, *11*, B113−B116.
(5) Trogadas, P.; Parrondo, J.; Mijangos, F.; Ramani, V. *J. Mater. Chem.* **2011**, *21*, 19381−19388.
(6) Trogadas, P.; Parrondo, J.; Ramani, V. *ACS Symp. Ser.* **2010**, *1034*, 187−207.
(7) Trogadas, P.; Parrondo, J.; Ramani, V. *Chem. Commun.* **2011**, *47*, 11549−11551.
(8) Prabhakaran, V.; Arges, C. G.; Ramani, V. *Proc. Natl. Acad. Sci. U.S.A.* **2012**, *109*, 1029−1034.
(9) Mauritz, K. A.; Moore, R. B. *Chem. Rev.* **2004**, *104* (10), 4535−4585.
(10) Borup, R.; Meyers, J.; Pivovar, B.; Kim, Yu, S.; Mukundan, R.; Garland, N.; Myers, D.; Wilson, M.; Garzon, F.; Wood, D.; Zelenay, P.; More, K.; Stroh, K.; Zawodzinski, T.; Boncella, J.; McGrath James, E.; Inaba, M.; Miyatake, K.; Hori, M.; Ota, K.; Ogumi, Z.; Miyata, S.; Nishikata, A.; Siroma, Z.; Uchimoto, Y.; Yasuda, K.; Kimijima, K.-I.; Iwashita, N. *Chem. Rev.* **2007**, *107* (10), 3904−3951.
(11) Aoki, M.; Uchida, H.; Watanabe, M. *Electrochem. Commun.* **2006**, *8* (9), 1509−1513.
(12) Bauer, F.; Denneler, S.; Willert-Porada, M. *J. Polym. Sci., Part B: Polym. Phys.* **2005**, *43*, 786.
(13) Patil, Y. P.; Seery, T. A. P.; Shaw, M. T.; Parnas, R. S. *Ind. Eng. Chem. Res.* **2005**, *44*, 6141.
(14) Inaba, M.; Yamada, H.; Tokunaga, J.; Tasaka, A. *Electrochem. Solid-State Lett.* **2004**, *7*, A474.
(15) Liu, W.; Zuckerbrod, D. *J. Electrochem. Soc.* **2005**, *152*, A1165.
(16) Teranishi, K.; Kawata, K.; Tsushima, S.; Hirai, S. *Electrochem. Solid-State Lett.* **2006**, *9*, A475.
(17) Madden, T.; Weiss, D.; Cipollini, N.; Condit, D.; Gummalla, M.; Burlatsky, S.; Atrazhev, V. *J. Electrochem. Soc.* **2009**, *156*, B657.
(18) Mittal, V. O.; Kunz, H. R.; Fenton, J. M. *J. Electrochem. Soc.* **2006**, *153*, A1755.
(19) Thompson, E. L.; Jorne, J.; Gasteiger, H. A. *J. Electrochem. Soc.* **2007**, *154*, B783.
(20) Inaba, M.; Kinumoto, T.; Kiriake, M.; Umebayashi, R.; Tasaka, A.; Ogumi, Z. *Electrochim. Acta* **2006**, *51*, 5746.
(21) Patil, Y. P.; Jarrett, W. L.; Mauritz, K. A. *J. Membr. Sci.* **2010**, *356* (1−2), 7−13.
(22) Patil, Y.; Sambandam, S.; Ramani, V.; Mauritz, K. *J. Electrochem. Soc.* **2009**, *156* (9), B1092−B1098.
(23) Trogadas, P.; Ramani, V., *J. Electrochem. Soc.* **2008**, *155*, B696−B703.
(24) Patil, Y. P.; Kulkarni, S. V.; Mauritz, K. A. *J. Appl. Polym. Sci.* **2011**, *121* (4), 2344−2353.